International Journal of GEOMATE, Oct., 2022, Vol.23, Issue 98, pp.179-188
ISSN: 2186-2982 (P), 2186-2990 (O), Japan, DOI: https://doi.org/10.21660/2022.98.3543
Geotechnique, Construction Materials and Environment

STRENGTH AND DEFORMATION PROPERTIES OF LIQUEFIED STABILIZED SOIL PREPARED BY VARIOUS CONDITIONS

Hung Khac Le[1] and *Yukihiro Kohata[1]

[1]Graduate School of Engineering, Muroran Institute of Technology, Japan

*Corresponding Author, Received: 02 Aug. 2022, Revised: 07 Sept. 2022, Accepted: 10 Oct. 2022

ABSTRACT: In Japan, Liquefied Stabilized Soil (LSS) is widely used as one of the effective utilization of excavated soil. LSS is a cement-treated soil classified as a slurry pre-mixed soil, which is easy to occur brittle failure and the addition of fiber content might improve the brittle behavior. Recently, various investigations into the strength and deformation properties of LSS with fiber were conducted. However, there is no comprehensive investigation of LSS with fiber under various combination conditions performed. Therefore, this study conducted a series of Consolidated-Undrained triaxial compression tests by a constant axial strain rate, with small unloading and reloading during the monotonic loading to investigate the effect of various densities and curing times on the mechanical properties of LSS. Also, the comparison of LSS mixed with the pulverized newspaper in the amounts of 0 and 10 kg/cm^3 cured laboratory and in-situ is discussed. Based on the test results, the effect of slurry density on the strength of LSS was found to be greater than the effect of curing time. The pre-peak behavior of the q~ε_a curve became more non-linear under the effect of changing slurry density, in contrast to the effect of curing time. Moreover, the damage degree of LSS with shearing becomes small with curing time, while it seems to be rather independent of slurry density. With in-situ LSS, the influence of curing time on the initial Young's modulus, E_0, is lower than the effect of slurry density.

Keywords: Liquefied stabilized soil, Fiber material, Slurry density, Cured in laboratory and in-situ, Triaxial Shear property

1. INTRODUCTION

Nowadays, environmental issues are arising from growing urbanization, especially in developing countries. Urban construction generates large amounts of construction waste soil that may not be appropriate for reuse in construction but may be harmful to the environment if not properly treated. Moreover, due to its small land area, the city confronts environmental issues such as a lack of final disposal sites and resource limitations, such as concerns about the potential exhaustion of mineral resources, and the waste and recycling problem has become a societal issue. This problem has received considerable attention. Therefore, finding a suitable use for recycled materials is desirable. Liquefied Stabilized Soil (LSS) [1] is one of a cement-treated soil, which improves the soil properties by the effect of cementation arising in an excavated soil mixed with cement-based solidification material and water, and has been extensively used in Japan. However, there is concern that the increased use of cement-based solidification material in LSS increases their strength and causes them to behave brittlely, reducing their seismic resistance. In order to improve brittle behavior, Kohata, Ito and Koyama in 2011 [2] proposed using pulverized newspaper as a fibered material to reinforce LSS, and conducted a series of unconfined and triaxial compression tests [2]. The study found that after the peak of the stress-strain curve, LSS mixed with a fibrous material had improved brittle behavior.

2. RESEARCH SIGNIFICANCE

Numerous studies have investigated the strength and deformation properties of LSS with fiber [2-8]. Nevertheless, no comprehensive investigation of LSS with fiber under various combination conditions has been performed. Especially the effect of various slurry densities and longer curing times on the strength and deformation properties of LSS cured in-situ conditions is not clear.

This study aims to investigate the strength and deformation properties of LSS prepared by various conditions. The effect of curing time and slurry density on the strength and deformation properties of LSS cured laboratory and in-situ were discussed based on the undrained triaxial compression test results for 48 cases.

3. TEST PROCEDURE

3.1 Test Material

In this study, the New Snow Fine Clay (NSF-Clay), which is a commercially cohesive soil, was used as the homogenous base material. The physical property of NFS-Clay is shown in Table 1. The Geoset 200 provided by Taiheiyo Cement Co., Ltd. was used as the cement-based solidification material. Newspapers were used as a fibrous

material, which was cut out to a suitable size with the office shredder. A cut newspaper was crushed with water by using a food processor. After drying it in a drying oven, untied it by hand, and it was pulverized again into smaller pieces like cotton wool. In other words, most contents of the fiber are composed of cellulose.

Table 1 Physical parameters of NSF-Clay

Physical parameters	Values
Particle density ρ_s (g/cm^3)	2.762
Liquid limit W_L (%)	60.15
Plastic limit W_P (%)	35.69
Plasticity index I_P	24.46
$M (=q_f/p'_f)$ [3]	1.20

3.2 Mixing and Specimen Preparation

There are two types of mixing methods for LSS, that is, the "slurry method" and the "adjusted slurry method". In this study, LSS was prepared by the "slurry method" because it is easier for preparation, in which NSF-Clay is mixed with an appropriate amount of water to produce a density-controlled slurry, which is then mixed with solidification material and fiber material.

In order to investigate the effect of various slurry densities on the strength and deformation of LSS reinforced fiber material, the basic slurry density was decided to be 1.280 g/cm^3, that is based on the standard mix proportion design figure [2], and the slurry density changing rate $D_{\rho f}$ (actual slurry density) / (basic slurry density) x 100 % was defined as, $D_{\rho f}$ = 100 % (ρ_f = 1.280 g/cm^3), $D_{\rho f}$ = 105 % (ρ_f = 1.344 g/cm^3) and $D_{\rho f}$ = 95 % (ρ_f = 1.216 g/cm^3), respectively. To achieve the desired slurry density, the density test was performed by measuring the mass of slurry poured into stainless steel container (AE mortar container) of 400 cm^3 in volume and the excess portion was cut off with a glass plate. After adjusting the slurry several times to obtain the required density, solidification material in the amount of 100 kg/m^3 was added to the slurry. The amount of fiber material added was referred to as being 10 kg/m^3 based on a previous study [2-8] (1.963 g/specimen). After adding the fiber material, LSS was mixed with a handy type mixer. Before filling the mold, the laboratory-cured specimens were deaired by the negative pressure of about -90 kPa for 30 minutes and put in a 50 x 100 mm commercial plastic mold with fabric tape on top for extra filling. After filling the container with treated soil, a plastic film was attached to the top edge. The excess portion of fill was trimmed off after 3 hours of curing. The top surface was flattened, re-covered with a polymer film, covered with a wet towel, and cured in moist air at 20±3 °C.

For the in-situ cured specimens, they were poured into isolated pits excavated in the campus grounds and allowed to cure for the prescribed days (42, 56, 80, and 126 days). Fig.1 illustrates a schematic diagram of the pits. After placement, the surface of LSS was covered with a polymer sheet and cured in-situ. Using a trimmer and straight edge, the LSS blocks were excavated and formed into cylindrical specimens in the laboratory. The programme of the undrained triaxial compression test is summarized in Table 2.

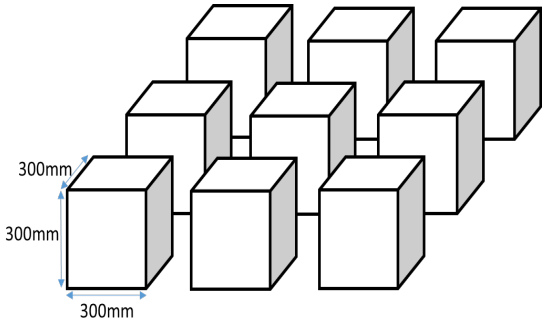

Fig.1 Schematic diagram of pits

3.3 Testing Method

In this study, a triaxial compression test apparatus with a pair of local deformation transducers (LDTs) [9] installed on each side of the specimen was used to measure axial displacement at the small strain level and to avoid the bedding errors caused by loose layers at the top and bottom edges of the specimen and filter paper compression. A dial gauge is used to determine the axial displacement when LDTs exceeded a measurable range. Fig.2 shows the triaxial compression test apparatus schematically. In this test, a digital servo motor, which enables to control of the axial strain

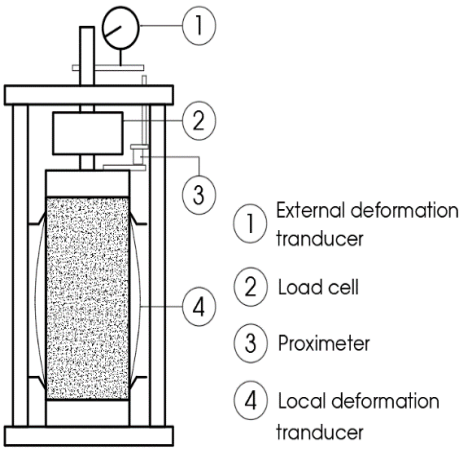

Fig.2 Schematic diagram of test apparatus

Table 2 Programme of undrained triaxial compression test

Test	Case ID	Specimen ID	Curing Time (days)	Slurry Density (g/cm^3)	Fiber Content (kg/ cm^3)	Cement content (kg/cm^3)	Curing condition
1(25)	S-42-1-In (out)	①	42	$D_{\rho f}$=1.216	Pc=0	100	Cured **laboratory** and **In-situ**
2(26)	S-56-1-In (out)		56				
3(27)	S-80-1-In (out)		80				
4(28)	S-126-1-In (out)		126				
5(29)	S-42-2-In (out)	②	42		Pc=10		
6(30)	S-56-2-In (out)		56				
7(31)	S-80-2-In (out)		80				
8(32)	S-126-2-In (out)		126				
9(33)	S-42-3-In (out)	③	42	$D_{\rho f}$ =1.344	Pc= 0		
10(34)	S-56-3-In (out)		56				
11(35)	S-80-3-In (out)		80				
12(36)	S-126-3-In (out)		126				
13(37)	S-42-4-In (out)	④	42		Pc=10		
14(38)	S-56-4-In (out)		56				
15(39)	S-80-4-In (out)		80				
16(40)	S-126-4-In (out)		126				
17(41)	S-42-5-In (out)	⑤	42	$D_{\rho f}$ =1.28	Pc=0		
18(42)	S-56-5-In (out)		56				
19(43)	S-80-5-In (out)		80				
20(44)	S-126-5-In (out)		126				
21(45)	S-42-6-In (out)	⑥	42		Pc=10		
22(46)	S-56-6-In (out)		56				
23(47)	S-80-6-In (out)		80				
24(48)	S-126-6-In (out)		126				

with high precision, and can ignore backlash when reversing the loading direction, was used for the loading device. The whole operation of the apparatus during the test was automatically controlled by PC software. The saturation of the specimen was achieved by the double negative pressure method which the de-aired water flowed through the specimen under a back pressure of 196 kPa. After isotropically consolidated for 15 hours under the effective confining pressure of 98 kPa, the specimen was sheared by undrained triaxial compression. To investigate the small strain deformation property, small unloading/reloading loops were applied on the pre-failure region of the stress-strain curve and axial strain rate of 0.054 % /min. The lowest speed of the loading system was set to record more data at a small strain level and it is also identical to the previous study [2-8].

4. RESULT AND DISCUSION

4.1 Stress-strain Relationships

4.1.1 Effect of slurry density

In order to investigate the effect of slurry density on the strength and deformation properties of LSS, the relationships between deviator stress q and axial strain ε_a based on a locally measured axial strain by LDTs with various slurry densities at 42 days of laboratory and in-situ curing are shown in Fig.3 and Fig.4. Fig.3 a) and Fig.4 a) show the q~ε_a relation up to ε_a =3.5 %. Also, Fig.3 b) and Fig.4 b) show at the small strain level up to 0.01 % for evaluating small strain stiffness. It is found that the change of slurry density influences significantly the strength of LSS both laboratory and in-situ at 42 days of curing. Fig.5 shows the relationship between maximum deviator stress q_{max} and the changing rate of slurry density at 42 days of laboratory and in-situ curing. By defining the average decreasing or increasing of q_{max} as (the value that decreased or increased in q_{max}) / (q_{max} with basic slurry density)×100 % [7], the average increasing rate in the laboratory and in-situ curing are shown to be about 40 % in case of the specimen with larger slurry densities, whereas the average decreasing rate in the laboratory and in-situ curing are shown to be 30 % and 14 % in case of that with lower slurry densities, respectively. This result shows that the strength of LSS cured in-situ decreased significantly compared to that of LSS cured laboratory. Therefore, it is considered that the quality of LSS reduces construction site when using LSS prepared by a lower slurry density to reduce the

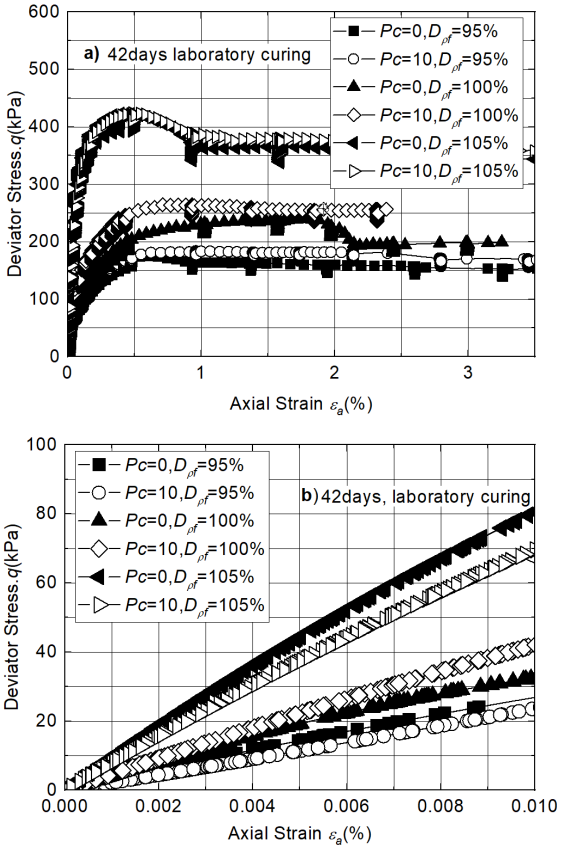

Fig.3 q vs ε_a relation of 42 days curing laboratory specimens; a) The relation up to 3.5 %, b) The relation up to 0.01 %

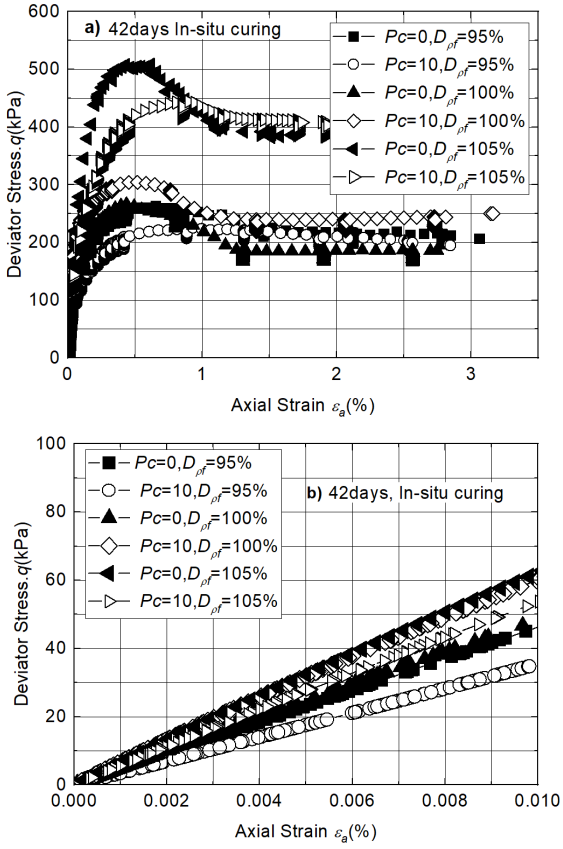

Fig.4 q vs ε_a relation of 42 days curing in-situ specimens; a) The relation up to 3.5 %, b) The relation up to 0.01 %

overburden pressure, then it should be careful. Moreover, the q_{max} of in-situ specimens substantially tends to be higher than that of laboratory specimens, and it is independent of slurry density. However, in Fig.4 b), the gradient of the q~ε_a relation at small strains for in-situ specimens are less than that of laboratory specimens as shown in Fig.3 b), whereas in Fig.4 a), the q_{max} of in-situ specimens for large slurry density is large than that of laboratory specimens. This indicates that when increasing slurry density at the laboratory, the stiffness at small strain increases compared to the other specimens that tend to only slightly increase at in-situ conditions. It is considered that the magnitude of viscous resistance appears to decrease with an increase in plasticity and water content at in-situ [10]. As a result, increases or decreases in slurry density have a greater influence on the stiffness of the LSS cured laboratory than when it is cured in-situ.

As the cement-based solidification material of LSS increases, the property of LSS becomes more brittle. However, when adding fiber material, in the q~ε_a curve after the peak, the value of q becomes nearly constant or slightly decreases in the majority of the cases. This indicates that by mixing fiber material, the brittleness property, ductile performance, and residual strength of LSS were significantly improved after the peak. This is verified by many previous studies [2-8]. From the test results in this study, it is found that the q_{max} of basic slurry density increases in LSS with fiber material (Pc=10) cured at both laboratory and in-situ. On the other hand, it is found that the q_{max} of high slurry density decreases in LSS with fiber material (Pc=10) cured in-situ compared to LSS without fiber material (Pc=0). It is considered that when adding fiber material and increasing slurry

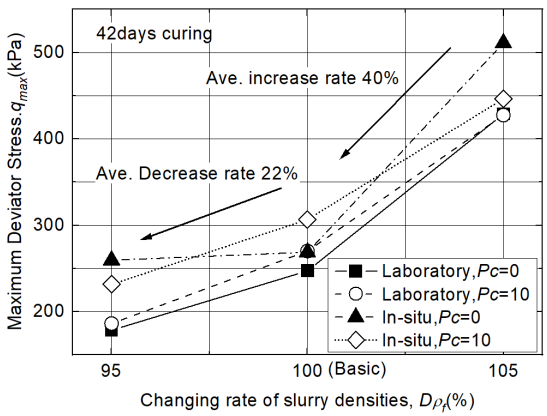

Fig.5 Relationship between q and changing rate of slurry densities

density, the cement-hydration process was delayed during the early curing stage due to decreasing water content and fluidity at in-situ.

In order to estimate the brittleness property after the peak, the brittleness index (I_B) [11] was defined in this study.

$$I_B = (q_{max}/q_{res}) - 1 \quad (1)$$

Where q_{max} is the maximum deviator stress and q_{res} is the residual deviator stress. As the value of the brittleness index I_B decreases and approaches zero, the failure behavior becomes increasingly ductile and the brittleness property is improved.

Fig.6 a) shows the comparison of the value of I_B for LSS without fiber material (Pc=0) and LSS with fiber (Pc=10). The I_B value of LSS with fiber (Pc=10) becomes roughly one-half of the value of I_B of LSS without fiber (Pc=0). In comparison to the basic slurry density ($D_{\rho f}$=100 %), the improvement effect of brittleness decreased with increasing slurry density in LSS of Pc=10 cured laboratory, but it improved significantly in LSS of Pc=10 cured in-situ as shown in Fig.6 b). This result can be seen as the most effective method to mix fiber into LSS with changing slurry density to improve the brittleness property, to increase ductile performance, and seismic resistance at the construction site, although there was a slight decrease in q_{max} value.

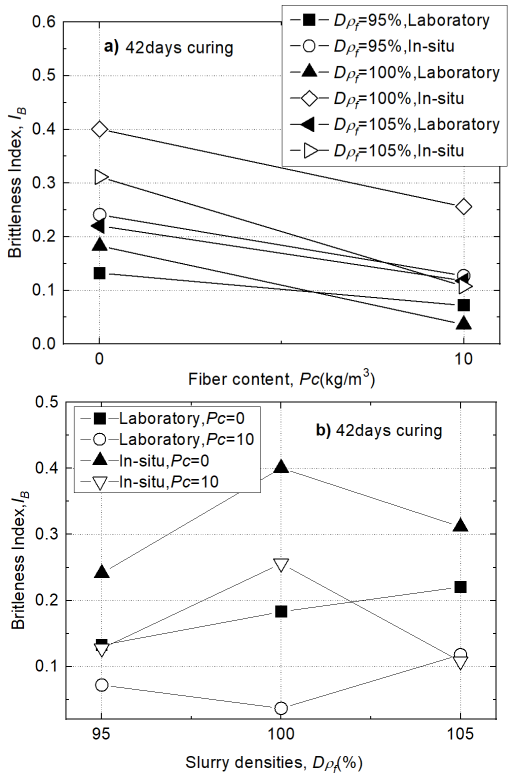

Fig.6 Relationships between I_B and a) fiber content, b) changing rate of slurry densities

4.1.2 Effect of curing time

The effect of curing time on strength and post-peak brittleness property of LSS in various conditions (amount of fiber material Pc, curing condition) was investigated. The relationship between q and ε_a up to ε_a=3.5 % based on LDTs measurement with the basic slurry density $D_{\rho f}$=100 % at prescribed curing time at the laboratory and in-situ is shown in Fig.7 and Fig.8. The figures show that the maximum deviator stress q_{max} increased with increasing curing time in most cases. Fig.9 shows the relationship between q_{max} and curing time, t by both logarithms. The $q_{max} \sim t$ relation is linear as $q_{max}=a\times(t)^n$ [12]. In both logarithm plots, the value of "n" represents the slope of the line obtained by a linear fit. The value of n becomes smaller than in cases of added fiber material (Pc=10) and cured in-situ. It means that the effect of aging on the increasing rate of the strength of LSS becomes small due to the addition of fiber material and curing at in-situ. Fig.10 shows the relationship between I_B and curing time. It is found that in the case of specimens cured laboratory, there was an increasing tendency of I_B with increasing curing time. The value of I_B for LSS with fiber

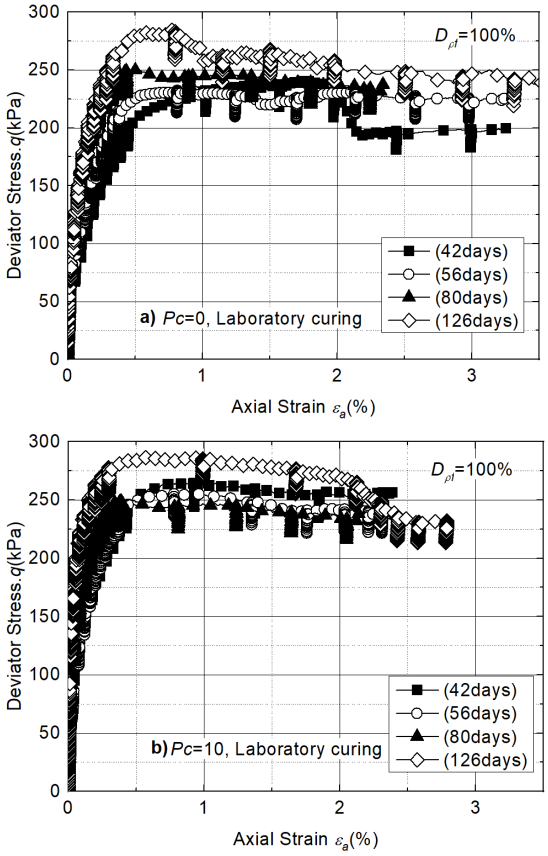

Fig.7 q vs ε_a relation with $D_{\rho f}$ =100%, Pc=0; a) Pc=0, Laboratory curing, b) Pc=10, Laboratory curing.

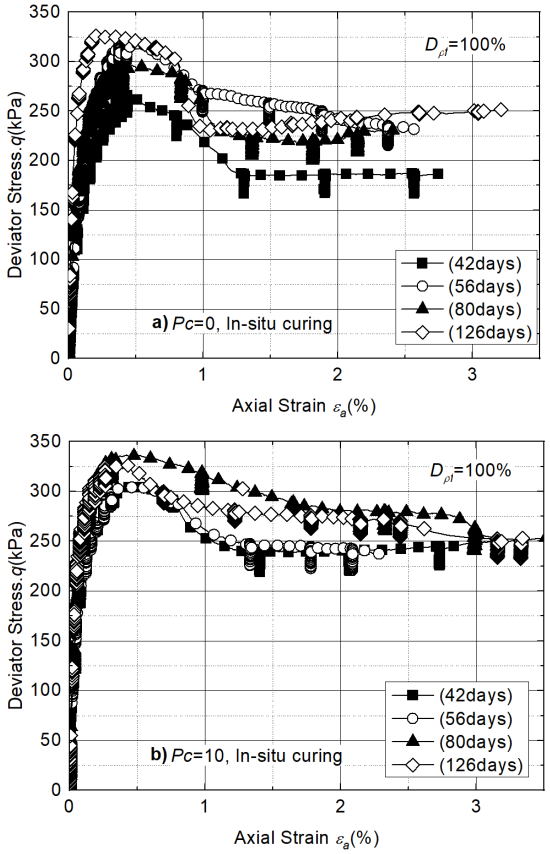

Fig.8 q vs ε_a relation with D_{pf}=100%, Pc=10; a) Pc=0, In-situ curing, b) Pc=10, In-situ curing.

material cured in-situ increases slightly and indicates nearly constant value at a long period of time. On the other hand, the decreasing tendency of I_B was found for LSS without fiber material cured in-situ. It is considered that the post-peak brittleness property decreases due to the increasing cementation effect with increasing of curing time. It is found that by adding fiber material into in-situ samples, the effect of aging on post-peak brittleness

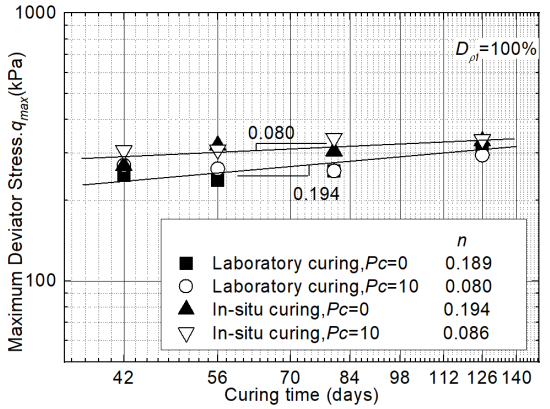

Fig.9 q_{max} *vs.* t relations

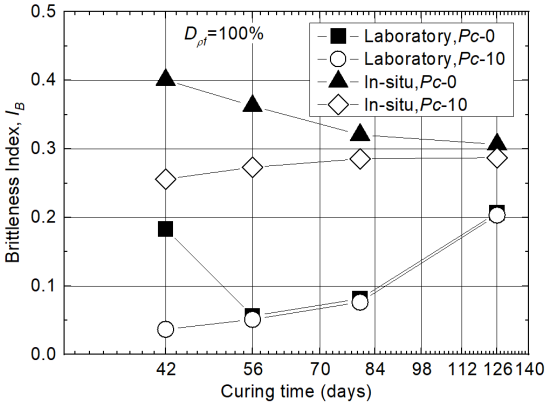

Fig.10 Brittleness index I_B vs. Curing time (days)

improvement is negligible when compared to other conditions.

4.2 Pre-failure deformation property

Various Young's moduli are defined as shown in Fig.11 in this study. The initial Young's modulus E_0 is defined as an initial stiffness at ε_a less than about 0.002 % measured with LDTs. It is different from the undamaged elastic Young's modulus. The E_{tan} is defined as a tangential gradient in q~ε_a curve. This value indicates the non-linearity of the deformation property in q~ε_a curve. The value of peak-to-peak secant modulus from an unload/reload cycle is defined as the equivalent Young's modulus, E_{eq} [13], as shown in Fig.11. The E_{50} value is obtained from the secant gradient between the coordinate origin and the point of q_{max}/2 on the q~ε_a curve.

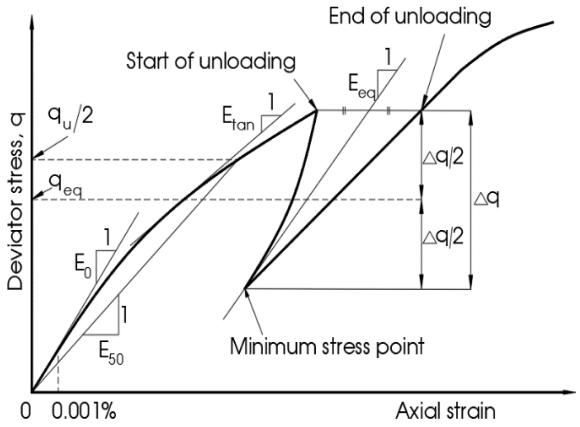

Fig.11 Definitions of E_0, E_{tan}, E_{eq}, E_{50}

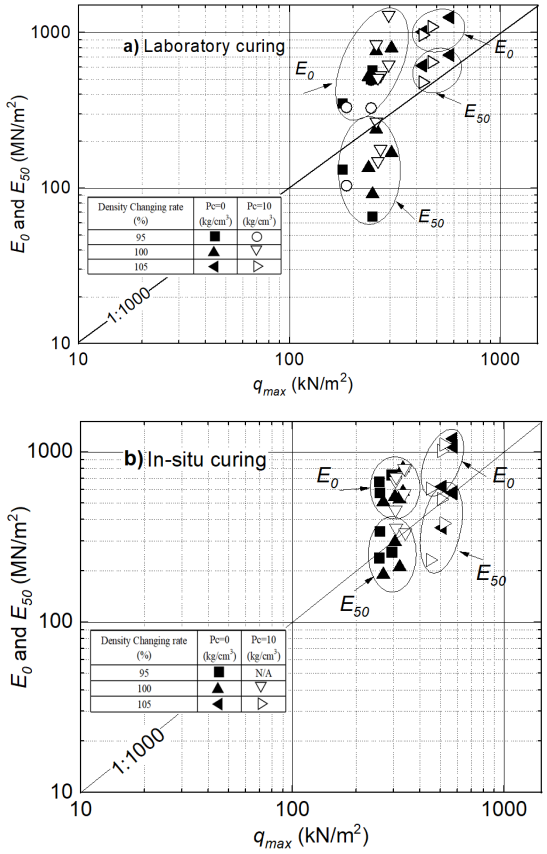

Fig.12 E_0, E_{50} *vs.* q_{max} relations; a) Laboratory curing, b) In-situ curing.

4.2.1 Relationships between Young's moduli E_0, E_{50}, and maximum deviator stress q_{max}

It is convenient to estimate the E_0 value from the q_{max}, because the accurate calculation of E_0 is so often much more difficult than that of q_{max}. Fig.12 shows E_0 and E_{50} ~ q_{max} relations. The figure shows that the relationship between E_0 and q_{max}, E_{50} and q_{max} are $E_0 \cong 1000\sim3000\times q_{max}$ and $E_{50} \cong 600\sim1100\times q_{max}$, irrespective of slurry density and curing time in most cases. However, the E_{50} value of LSS cured in-situ with low slurry density is large in compared with LSS cured laboratory, while the E_{50} value of LSS cured in-situ with high slurry density is smaller than laboratory ones. This result can be seen that the pre-failure $q\sim\varepsilon_a$ curve seemed to be more non-linear in LSS cured laboratory with low slurry density and in LSS cured in-situ with high slurry density than in others. Fig.13 shows the effect of curing time on E_0. The increasing trend of E_0 for laboratory curing is observed at a relatively small curing period compared to E_0 for in-situ curing. That is, it is considered that the appearance of initial stiffness for in-situ curing becomes to delay compared to that for laboratory curing due to factors of curing temperature, humidity etc. at in-situ.

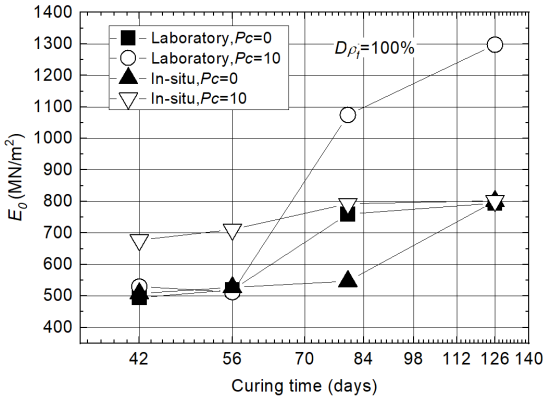

Fig.13 E_0 vs. Curing time (days)

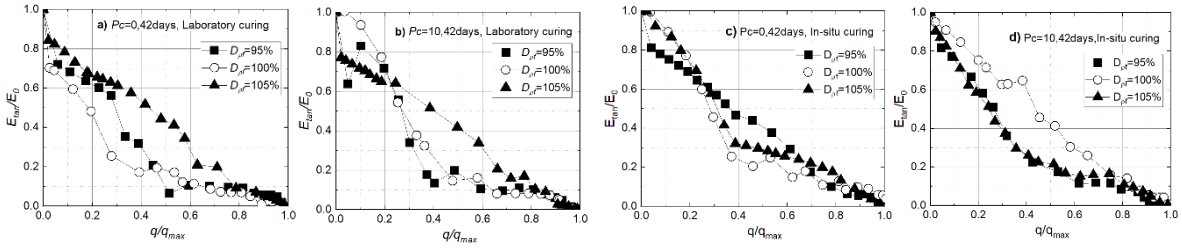

Fig.14 Effect of slurry density on E_{tan}/E_0 vs. q/q_{max} relations; a) Pc = 0, 42 days, Laboratory curing, b) Pc = 10, 42 days, Laboratory curing , c) Pc = 0, 42 days, In-situ curing, d) Pc = 10, 42 days, In-situ curing.

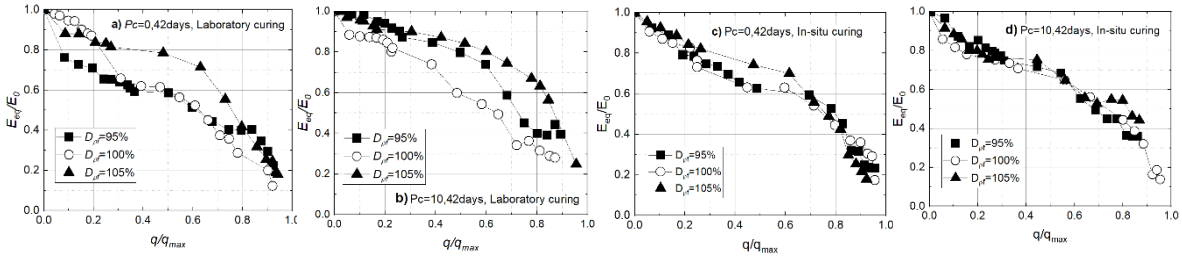

Fig.15 Effect of slurry density on E_{eq}/E_0 vs. q/q_{max} relations; a) Pc = 0, 42 days, Laboratory curing, b) Pc = 10, 42 days, Laboratory curing , c) Pc = 0, 42 days, In-situ curing, d) Pc = 10, 42 days, In-situ curing.

4.2.2 Effect of slurry density

The relationship between the tangent Young's modulus normalized by the initial Young's modulus (E_{tan}/E_0) and the deviator stress normalized by the maximum deviator stress (q/q_{max}) in different cases is shown in Fig.14. These relations indicate the non-linearity of pre-failure deformation property and the degree of non-linearity can be compared normalizing the tangent Young's modulus and the deviator stress. Also, the relationship between the equivalent Young's modulus normalized by the initial Young's modulus (E_{eq}/E_0) and the deviator stress normalized by the maximum deviator stress (q/q_{max}) in different cases is shown in Fig.15. These relations indicate the degree of damage with shear in pre-failure deformation property.

In the case of in-situ curing as shown in Figs. 14 c) and d), for Pc=0, the rate of decrease of E_{tan}/E_0 with shear is similar regardless of the slurry density up to q/q_{max}=0.4. The decreasing trend of E_{tan}/E_0 is largest when $D_{\rho f}$ = 100 %. On the other hand, for Pc=10, no effect of slurry density on the E_{tan}/E_0 to q/q_{max} relations is seen, and the curves are nearly identical. In the case of laboratory curing as shown in Figs.14 a) and b), the rate of decrease of E_{tan}/E_0 with shear is significantly smaller for $D_{\rho f}$ = 105 % than for $D_{\rho f}$ = 95 % and 100 %, regardless of whether the fiber material is mixed or not. It was also observed that the decreasing trend of E_{tan}/E_0 for $D_{\rho f}$ = 95 % at ranges greater than q/q_{max}= 0.4 is increasing. In in-situ curing, the appearance of strength is slower than in laboratory curing due to factors such as curing temperature and humidity. Then, it is assumed that the effects of mixing a fiber material and the changing of slurry density were not appeared noticeably in the curing time at 42 days. On the other hand, it is considered that the effect of slurry density on the E_{tan}/E_0~q/q_{max} relations was appeared more significantly for $D_{\rho f}$ = 105 % in the curing time at 42 days, because the curing environment is controlled in laboratory curing.

As the shear deformation increases due to the damage to the micro-structure and the increase in viscous-plastic effect as well, the unload/reload stress-strain curves become more open when evaluated at shear stress levels closer to the peak stress state. That is, if E_{eq}/E_0 is less than 1.0, the E_{eq} value may become less than the corresponding E_0 value [8].

In the laboratory curing as shown in Figs. 15 a) and b), there is the effect of slurry density on the E_{eq}/E_0~q/q_{max} relations, regardless of the amount of fiber material. Especially, the degree of damage for $D_{\rho f}$ = 105 % is the smallest. On the other hand, in the in-situ curing as shown in Figs. 15 c) and d), it is not seen that the effect of slurry density and amount of fiber material on the degree of damage with shear is not seen significantly.

As a result, it is found that the effect of the slurry density on the LSS with fiber material cured in-situ is much more non-linear in the pre-failure deformation, and more ductile in the post-peak deformation. It is proposed to use LSS with varying slurry densities to increase seismic resistance and reduce overburden loads on construction sites.

4.2.3 Effect of curing time

The influence of curing time on the non-linearity of the stress-strain relationship in the pre-failure region and the effect of the shear stress during aging on the non-linearity are analyzed as shown in Fig. 16 and Fig. 17. In the E_{tan}/E_0 ~q/q_{max}

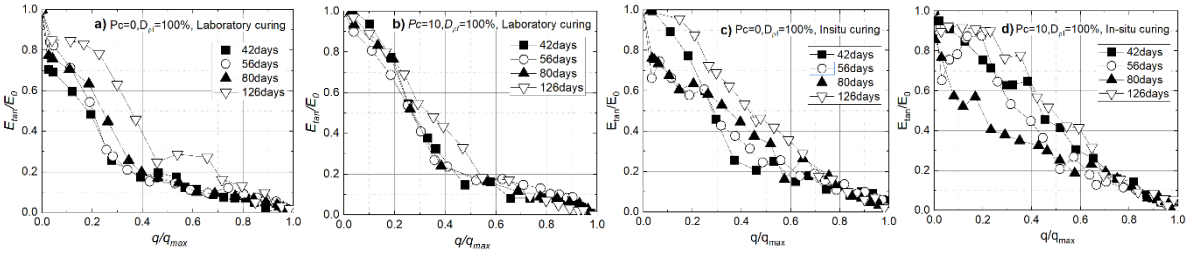

Fig.16 Effect of curing time on E_{tan}/E_0 vs. q/q_{max} relations; a) Pc = 0, 42 days, Laboratory curing, b) Pc = 10, 42 days, Laboratory curing , c) Pc = 0, 42 days, In-situ curing, d) Pc = 10, 42 days, In-situ curing.

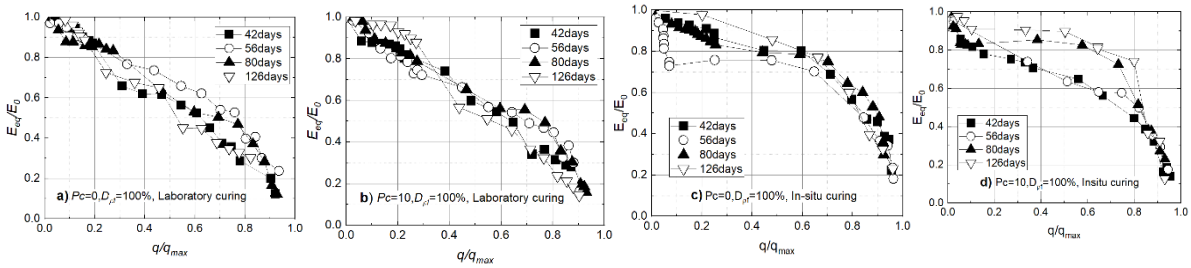

Fig.17 Effect of curing time on E_{eq}/E_0 vs. q/q_{max} relations; a) Pc = 0, 42 days, Laboratory curing, b) Pc = 10, 42 days, Laboratory curing , c) Pc = 0, 42 days, In-situ curing, d) Pc = 10, 42 days, In-situ curing.

relations in Figs.16 a) and c), the value of E_{tan}/E_0 is not decreased up to around q/q_{max} = 0.2 with increasing curing time for LSS in both the laboratory and in-situ cases. The decreasing tendency of E_{tan}/E_0 with increasing of q/q_{max} in more than q/q_{max} = 0.4 is large at a long time of curing (126 days) in both cases. However, by adding fiber material into specimens cured in-situ, the non-linearity of the pre-failure $q\sim\varepsilon_a$ curve seems to become rather independent of curing time in Figs.16 b) and d). Moreover, it can be seen that it is difficult to predict the influence of curing time on the non-linearity of the pre-failure $q\sim\varepsilon_a$ curve due to uncontrolled environmental conditions. For this result, it is considered necessary to conduct further work that controls more factors influencing specimens in the coming time.

Figs.17 a) and b) show that the degree of damage with shear for laboratory curing in both cases of LSS without fiber material and with ones seems to become independent of curing time. Meanwhile, the E_{eq}/E_0 for in-situ curing as shown in Figs.17 c) and d) is larger than when compared with laboratory curing. In particular, by mixing fiber material at in-situ, the remarkable effect of curing time on the $E_{eq}/E_0\sim q/q_{max}$ relations is large, as shown in Fig.17 d). The value of E_{eq}/E_0 increases remarkably as the curing time increases. It is considered that this is due to a decrease of the viscous component of deformation during unload / reload cycle with shear as the curing time increases and an increase of the elastic component of strain by increasing of curing time in in-situ curing. This property is similar to that of cement-treated gravelly soil [10].

5. CONCLUSION

Based on the results of a series of undrained triaxial compression tests on LSS mixed with and without fiber material, the following conclusions were obtained.

1) The slurry density had a considerable effect on the strength of LSS, with increasing density resulting in a 40 % rise in value of q_{max} and lowering density resulting in a 20 % drop in value of q_{max} when the density was changed at the same rate.

2) According to the brittleness index, the brittle properties of LSS were improved significantly about twice by adding fiber material.

3) The relationship between the $\log(q_{max})$ and $\log(t)$ is linear. It seems that $q_{max}=a\times(t)^n$ is approved to the relation between q_{max} and curing time, t of cement-treated soil including LSS.

4) In case of in-situ curing, the effect of curing time on the increasing rate of strength is small when compared to LSS without fiber material cured laboratory. The appearance of cementation was considered to be delayed due to adding fiber material and increasing water content at in-situ.

5) The relationship of $E_0\cong1000\sim3000\times q_{max}$ and $E_{50}\cong600\sim1100\times q_{max}$ irrespective of slurry density and curing time in almost cases is approved to the relationship between E_0 and q_{max} of cement-treated soil including LSS.

6) The effect of curing time on the initial Young's modulus, E_0, is smaller than the effect of slurry density with LSS cured in-situ. In particular, the E_0 value is more sensitively changed by the slurry density with LSS cured laboratory.

7) The slurry density has a substantial influence on the stress-strain relationships of LSS with fiber material cured in-situ**.** With increasing slurry density, the pre-failure stress-strain relation becomes more non-linear and the post-peak stress-strain relation becomes more ductile, while q_{max} decreases slightly. Furthermore, the influence of shear stress level on the degree of damage appears to be independent of slurry density.

8) By adding fiber material into LSS cured in-situ, the non-linearity of pre-failure $q\sim\varepsilon_a$ curve seems to become rather independent of curing time, the effect of curing time on the post-peak deformation is negligible, while the effect of curing time on the degree of damage is found to be largely due to a decrease in the viscous component of deformation and an increase of the elastic component of strain.

9) Since uncontrolled environmental factors make it much more difficult to predict the strength and deformation behavior of LSS cured in-situ. It is considered necessary to conduct further work that controls more factors influencing specimens

6. ACKNOWLEDGMENTS

The authors express deep gratitude to Mr. Moteki, Mr. Onodera (formerly, graduate and undergraduate student), and Ms. Watanabe, Mr. Okada, and Ms. Xi (undergraduate student of Muroran Institute of Technology) for sample preparation, experiments and data analysis.

This work was supported by JSPS KAKENHI Grant Number JP19K04590 (Grant-in-Aid for Scientific Research(C))

7. REFERENCES

[1] Kuno G., eds, Liquefied stabilized soil method Recycling technology of construction-generated soil and mud, *Gihodo publication*, 1997 (in Japanese).

[2] Kohata Y., Ito, K., and Koyama Y., Influence of additive amount of cement solidification on agent on mechanical characteristics of Liquefied Stabilized Soil mixed with fibered material, Japanese Geotechnical Society Hokkaido Branch Technical Report Papers, Vol.51, 2011,

131-136, (in Japanese).
[3] Kawaguchi T., Mitachi T., and Shibuya S., Quantifying deformation modulus of reconstituted clays at small strains, Japanese Journal of JSCE, No.631/III-49, 1999, 179-191(in Japanese).
[4] Duong Hung Q., Kohata Y., Omura S., and Ozaki K., Strength and deformation characteristics of liquefied stabilized soil reinforced by fiber material prepared at laboratory and field, Geosynthetics Engineering Journal, Vol.29, 2014, pp.33-40.
[5] Do Anh T., Kohata Y., and Sasaki M., Effect of slurry density on triaxial compressive properties for liquefied stabilized soil reinforced with fiber material, Geosynthetics Engineering Journal, Vol.33, 2018, pp.15-22.
[6] Do Anh T., Kohata Y., Reduction of Vehicle-Induced Vibration Using Liquefied Stabilized Soil, Journal of Geosynthetics, Vol.34, 2019, 123-128.
[7] Cui Y., and Kohata Y., Influence of cement solidification agent and slurry density on mechanical property of liquefied stabilized soil, International Journal of GEOMATE, Vol.19, Issue 73, 2020, 177-184.
[8] Pham Vuong Q., Kohata Y., Effect of Liquefied Stabilized Soil as Backfilling Material on the Building under Seismic Condition, International Journal of GEOMATE, Vol.20, Issue 77, 2021, 155-162.
[9] Goto S., Tatsuoka F., Shibuya S., Kim Y-S., and Sato T., A simple gauge for local small strain measurements in the laboratory, Soils and Foundations, Vol. 31, No. 1, 1991, 169-180.
[10] Tatsuoka F., and Kongsukprasert L., Small strain stiffness and non-linear stress-strain behavior of cement-mixed gravelly soil, Soils and foundations, Vol.47, No.2, 2007, 375-394.
[11] Consoli NC., Montardo JP., Prietto PDM., and Pasa GS., Engineering behavior of a sand reinforced with plastic waste, J Geotech and Geo Environ Eng, Vol. 128, Issue 6, 2002, 462-472.
[12] Kohata Y., Tsushima H., Effect of fibered material mixing in liquefied stabilized soil on triaxial shear characteristics, Proc. of the 39th Japan National Conference on Geotechnical Engineering, 2004, pp.721-722 (in Japanese).
[13] Tatsuoka F., and Kohata Y., Stiffness of hard soils and soft rock in engineering aplications, Pre-failure deformation of Geomaterial, Balkema, Vol.2, 1995, 1030-1035.